

Structure and Stereodynamics of Aryldiimino Derivatives

Lodovico Lunazzi, Michele Mancinelli, and Andrea Mazzanti*

Department of Organic Chemistry "A. Mangini", University of Bologna,
Viale Risorgimento 4, Bologna 40136, Italy

mazzand@ms.fci.unibo.it

Received January 22, 2010



Nitrogen inversion

Ar-N rotation

Aromatic diimino derivatives, having two N=CPh₂ moieties bonded at the 1,8 positions of the anthraquinone, anthracene, biphenylene, and naphthalene rings, have been investigated by variable-temperature NMR spectroscopy, X-ray diffraction, and DFT calculations. In all the compounds, the imino substituents are essentially orthogonal to the aromatic plane and the phenyl groups bonded to the C=N carbons are diastereotopic (i.e., cis or trans to the aromatic N-substituent of the N=C moiety). The barriers for the cis/trans interconversion of the phenyl groups by planar nitrogen inversion have been determined. In the cases of anthracene and anthraquinone derivatives, the presence of syn and anti conformers was detected, and their interconversion barriers, due to the Ar-N rotation, were measured. At very low temperature, restricted rotations of the phenyl groups, displaying barriers in the range 4.8–6.9 kcal mol⁻¹, were also observed for all compounds: the barriers for the rotation of the cis were found to be larger than for the trans phenyl groups.

Introduction

Imines and diimine metal complexes are widely used for enantioselective synthesis (salen complexes),¹ tandem reactions,² coupling reactions,³ and olefin polymerization.⁴ Imines themselves (both as chiral or achiral substrates) are employed as precursors of active species in organocatalytic reactions like hydroxylation,⁵ epoxidation,⁶ and aziridination.⁷ A conformationally chiral diimine was recently observed in the solid state in its racemic form.⁸ In solution,

however, imines are known to undergo stereodynamic processes that involve the trigonal nitrogen atom coplanar to the atoms to which it is bonded. NMR spectroscopy is a convenient technique to investigate stereodynamic processes of this type, and thus, it has been widely applied for investigating the dynamic behavior of imines.⁹ In principle, there are two possible processes that might occur in imines, i.e., rotation about the C=N double bond and inversion of the planar nitrogen atom (sometimes referred to as lateral shift). There is a widespread agreement that the latter should require less energy,^{9a} especially in *N*-arylimines where the nitrogen inversion route is facilitated by conjugation involving the nitrogen lone pair and aryl moiety.

When two hindered imino substituents are bonded to an aromatic scaffold there are both conjugative and steric effects that need to be considered. Twisting the imino group out of the aromatic scaffold plane increases the conjugation

(1) McGarrigle, E. M.; Gilheany, D. G. *Chem. Rev.* **2005**, *105*, 1563–1602. Darensbourg, D. J. *Chem. Rev.* **2007**, *107*, 2388–2410. Cozzi, P. G. *Chem. Soc. Rev.* **2004**, *33*, 410–421. Katsuki, T. *Chem. Soc. Rev.* **2004**, *33*, 437–444.

(2) Du, H.; Ding, K. *Org. Lett.* **2003**, *5*, 1091–1093.

(3) Nelana, S. M.; Cloete, J.; Lisensky, G. C.; Nordlander, E.; Guzey, I. A.; Mapolie, S. F.; Darkwa, J. *J. Mol. Catal. A* **2008**, *285*, 72–78. Weissman, H.; Milstein, D. *Chem. Commun.* **1999**, 1901–1902.

(4) Makio, H.; Fujita, T. *Acc. Chem. Res.* **2009**, *42*, 1532–1544 and reference cited therein

(5) Brodsky, B. H.; Du Bois, J. *J. Am. Chem. Soc.* **2005**, *127*, 15391–15393.

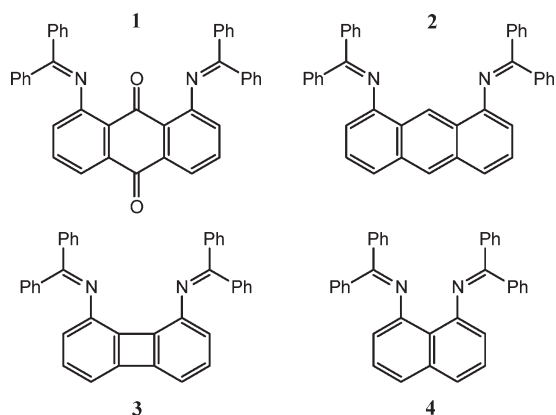
(6) Prieur, D.; El Kazzi, A.; Kato, T.; Gornitzka, H.; Baceiredo, A. *Org. Lett.* **2008**, *10*, 2291–2294.

(7) Müller, P.; Fruit, C. *Chem. Rev.* **2003**, *103*, 2905–2919.

(8) Glagovich, N. M.; Reed, E. M.; Crundwell, G.; Updegraff, J. B. III; Zeller, M.; Hunter, A. D. *Acta Crystallogr. E* **2005**, *E61*, 1251–1253.

(9) (a) For a comprehensive review on this subject, see: Jennings, W. B.; Wilson, V. E. In *Acyclic Organonitrogen Stereodynamics*; Lambert, J. B.; Takeuchi, Y., Eds.; VCH Publishers: New York, 1991; Chapter 6, pp 155–243 and references cited therein. (b) Dalla Cort, A.; Gasparrini, F.; Lunazzi, L.; Mandolini, L.; Mazzanti, A.; Pasquini, C.; Pierini, M.; Rompietti, R.; Schiaffino, L. *J. Org. Chem.* **2005**, *70*, 8877–8883.

CHART 1



between the sp^2 lone pair of the nitrogen and the aromatic system, but at the same time, the conjugation with the $C=N$ π system is lost. On the other hand, the $C=N$ π system can develop a good conjugation with the phenyls bonded to imine carbon. The final geometry might be therefore driven mainly by steric factors. When the plane of the $N=C$ moieties is nearly orthogonal to the aromatic plane, syn and anti forms should be, in principle, detectable. Depending on the height of their interconversion barriers, these forms can be considered either stereolabile conformers or configurationally stable isomers. In the present paper, a number of aromatic systems, bearing two equal imino substituents in two peri positions, have been investigated (see Chart 1). The use of different aromatic scaffolds makes it possible to modulate the distance between the two nitrogens, and the presence of two phenyl groups bonded to the sp^2 carbons of the $C=N$ group makes these imino derivatives hindered enough as to fulfill the conditions for a nonplanar structure.

Results and Discussion

In the anthraquinone derivative **1** each of the four ^{13}C lines of the phenyl carbons (three CH and one quaternary) broadens on cooling below ambient temperature and eventually splits into two lines of equal intensity at -45 °C. In Figure 1, the temperature dependence of one of the CH signals of the phenyl groups is displayed as an example: the rate constants obtained from the accompanying line shape simulation allowed us to obtain a free energy of activation (ΔG^\ddagger) of 13.4 kcal mol $^{-1}$ (Table 1). This value corresponds to the barrier required to freeze the planar inversion of the sp^2 nitrogen: DFT calculations actually support this hypothesis (the linear transition state is calculated to be 10.6 kcal mol $^{-1}$ above the ground state energy, as in Table 1). In such a situation, the two phenyl rings within each $Ph_2C=N$ moiety become, in fact, diastereotopic in that they adopt cis and trans dispositions with respect to the anthraquinone moiety, thus making anisochronous the corresponding NMR signals.

On further lowering the temperature the effects of a second process are observed, apparently affecting all of the signals but more conveniently followed by monitoring the 1H spectrum of the anthraquinone moiety. As shown in Figure 2, the doublet ($J = 8.1$ Hz) of the hydrogens in positions 2,7 (assigned by 2D-HMBC) broadens below -50 °C and splits into two doublets with a 94:6 ratio below -100 °C, the corresponding barrier being 9.2 kcal mol $^{-1}$ (Table 1). This

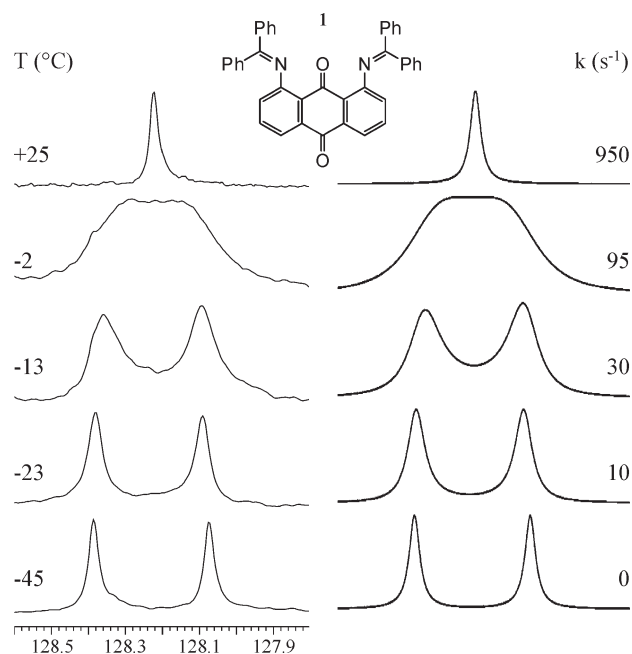


FIGURE 1. (Left) Temperature dependence of the ^{13}C signal (150.8 MHz in CD_2Cl_2) of one of the phenyl CH carbons of **1**, showing the effects of the sp^2 N-inversion process. (Right) Computer simulation obtained with the rate constants indicated.

TABLE 1. Experimental and DFT-Computed Barriers (kcal mol $^{-1}$) of Dynamic Processes in Compounds **1–4**

compd	N-inversion		Ar–N rotation		Ph rotation	
	exptl	computed	exptl	computed	exptl ^a	computed
1	13.4	10.6	9.2	8.1	5.8 ^b	4.9, ^b 4.8 ^c
2	16.2	15.1	5.8	3.9	5.4, ^c 4.8 ^b	6.1, ^c 5.7 ^b
3	17.3	13.7		2.7	5.6 ^b	5.2, ^c 5.2 ^b
4	16.6	15.5		9.8	6.9, ^c 5.4 ^b	7.6, ^c 6.9 ^b

^aDue to spectral crowding these values could be determined only at the coalescence temperature. ^bPair of phenyl groups trans to the aromatic scaffold (*E*). ^cPair of phenyl groups cis to aromatic scaffold (*Z*).

process is due to the restricted rotation about the *N*-anthraquinone bond which gives rise to conformers with the $Ph_2C=N$ moieties nearly orthogonal to the anthraquinone, corresponding to the syn and anti structures of Figure 3. The DFT calculations indicate, likewise, that the barrier for the Ar–N rotation of **1** is expected to be lower than that for the planar nitrogen inversion, the computed values being 8.1 and 10.6 kcal mol $^{-1}$, respectively (Table 1).

The same calculations predict that the syn conformer should be more stable than the anti by 0.7 kcal mol $^{-1}$ (Figure 3). Such an assignment is further supported by X-ray diffraction of **1** that shows how the imino moieties are nearly orthogonal to the anthraquinone ring and that the syn structure is actually adopted: the computed geometry for the syn conformer is very close to that obtained experimentally (Figure 3), and this shows that the computational tool employed is suitable to tackle this problem.

It is somewhat surprising that the apparently more hindered syn conformer is more stable than the less hindered anti. This depends on a most delicate balance between a variety of attractive and repulsive interactions that cannot be rationalized by means of a simple, intuitive argument: this complex situation is satisfactorily accounted for solely

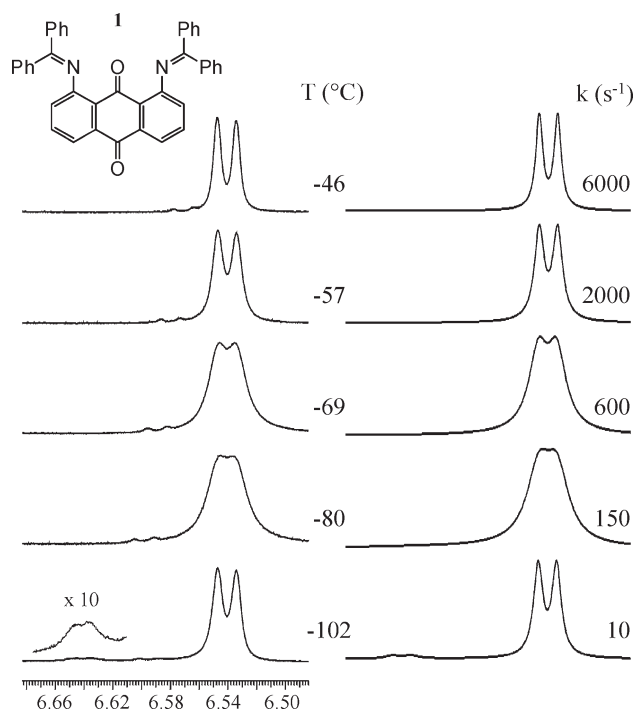


FIGURE 2. (Left) Temperature dependence of the ^1H signal (600 MHz in CD_2Cl_2) of the hydrogens in positions 2,7 of the anthraquinone moiety of **1**, showing the effects of the interconversion process between the syn and anti conformers by Ar–N rotation. The signal of the latter (6%) has been increased 10 times in the inset of the $-102\text{ }^\circ\text{C}$ trace. (Right) Computer line shape simulation obtained with the rate constants indicated, corresponding to the syn/anti exchange.

by appropriate DFT computations. In order to explore the possible existence of motions with even smaller barriers, a solvent which could reach temperatures much lower than $-100\text{ }^\circ\text{C}$ (as, for instance, CDFCl_2) had to be used. As expected on the basis of the previous investigations in CD_2Cl_2 , the ^1H spectrum in CDFCl_2 also exhibits, at $-40\text{ }^\circ\text{C}$, diastereotopic phenyl groups owing to the restricted sp^2 N-inversion.

On further lowering the temperature, the anthraquinone signals of the hydrogens in positions 2,7 and 4,5 broaden and eventually split at $-120\text{ }^\circ\text{C}$ into two unequally intense signals, due, as previously mentioned, to the restricted N-anthraquinone rotation generating syn and anti conformers.

Contrary to that observed in CD_2Cl_2 (where the corresponding ratio was 94:6), here the ratio between the upfield and downfield doublets is about 65:35 (Figure 4). This change of proportions agrees with the assignment of the more intense signal to the syn conformer. The latter, in fact, has a computed dipole moment (3.76 D) larger than the anti (3.30 D) and thus is expected to reduce its proportion (in the present case from 94% to 65%) in a solvent like CHFCl_2 (dipole moment^{10a} 1.34 D), which is less polar than CH_2Cl_2 (dipole moment^{10b} 1.60 D).

When the temperature is further lowered, the upfield major signals of the syn conformer (7.86 ppm for H4,5 and 6.65 ppm for H2,7) broaden below $-130\text{ }^\circ\text{C}$ and split, at $-155\text{ }^\circ\text{C}$, into two signals in a 55:45 proportion, the separations being

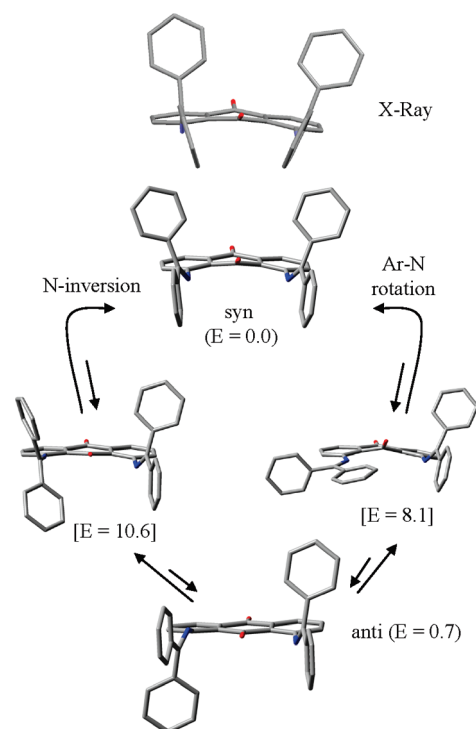


FIGURE 3. (Top) X-ray diffraction structure of **1**. Underneath are shown the two possible pathways with the corresponding transition states connecting the syn and anti conformers (the theoretically calculated energy values are in kcal mol^{-1} and the square brackets indicate the transition states).

0.11 and 0.03 ppm, respectively. This feature, on the contrary, does not occur in the downfield minor signals of the anti conformer (7.97 for H4,5 and 6.74 ppm for H2,7) that remain single signals (Figure 4). This indicates that the syn conformer comprises two unequally populated forms whereas the anti conformer does not. In addition, the signal due to the four ortho hydrogens of the pair of diastereotopic phenyl groups in a trans relationship to anthraquinone¹¹ splits, at $-120\text{ }^\circ\text{C}$, owing to the presence of the syn and anti conformers. However, when cooled to $-155\text{ }^\circ\text{C}$, the additional 55:45 splitting mentioned above for the syn anthraquinone signals is not observed, being obscured by a line broadening that eventually splits both the syn and anti ortho signals of the phenyl in the trans position into two equally intense signals (corresponding each to two hydrogens), with a very large separation (approximately 0.7 ppm).¹² Since such an effect is detected for the trans phenyl signals but not for the anthraquinone signals it is attributable to

(11) These signals are due to the four ortho hydrogens of the pair of phenyl groups (indicated as blue in Figure 4) in a trans relationship to the anthraquinone moiety. This assignment was ascertained on the basis of a NOE experiment at $-50\text{ }^\circ\text{C}$ (where the sp^2 N-inversion is frozen) by irradiating the anthraquinone signals of the hydrogens in position 2,7 (indicated as red in Figure 4). An enhancement was observed for the signals of the diastereotopic pair of phenyl groups at 7.7–7.3 ppm, indicating that these signals correspond to the pair of phenyl groups cis to the anthraquinone moiety. As a consequence, the dynamic effects we observed involve the ortho signals of the pair of diastereotopic phenyls trans to anthraquinone.

(12) In the $-155\text{ }^\circ\text{C}$ spectrum the ortho signals corresponding to two hydrogens are visible only on the left side of the spectrum (at about 8.1 ppm, as in Figure 4), whereas the corresponding companion on the right side is overlapped by a number of other signals. Thus, the mentioned separation of approximately 0.7 ppm of the diastereotopic ortho signals was obtained by doubling the separation between the averaged signals due to four hydrogens (see the spectrum at $-120\text{ }^\circ\text{C}$) and the left side signal due to two hydrogens (see the spectrum at $-155\text{ }^\circ\text{C}$).

(10) (a) Fuoss, R. M. *J. Am. Chem. Soc.* **1938**, *60*, 1633–1637. (b) Richardi, J.; Fries, P. H.; Krienke, H. *J. Phys. Chem. B* **1998**, *102*, 5196–5201.

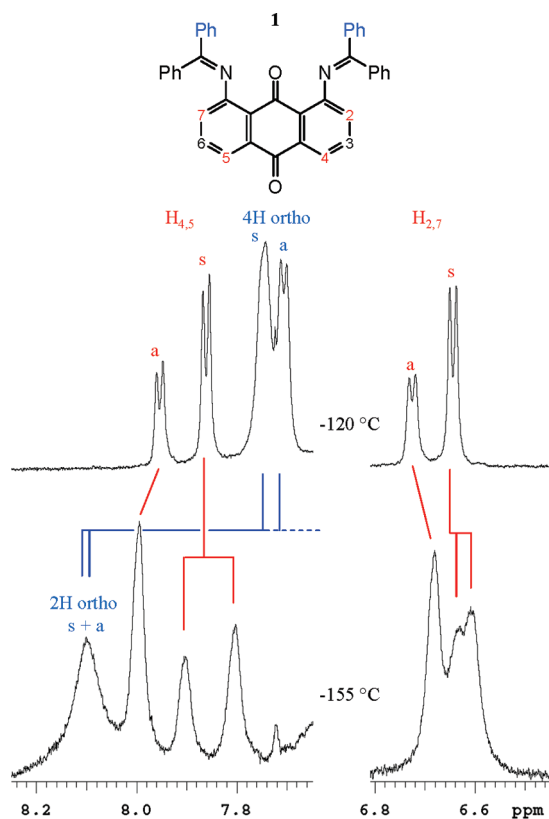


FIGURE 4. (Top) Portion of the ^1H spectrum of **1** (600 MHz in CDCl_2 at $-120\text{ }^\circ\text{C}$) showing the anthraquinone signals of $\text{H}_{2,7}$ and $\text{H}_{4,5}$ (in red) as well as the signal of the four ortho hydrogens of the pair of diastereotopic phenyl groups trans to the anthraquinone moiety (in blue). These signals are all split in a 65:35 ratio corresponding to syn (s, major) and anti (a, minor) conformer. (Bottom) The same spectrum at $-155\text{ }^\circ\text{C}$ showing additional splitting (55:45 ratio) of the anthraquinone signals in the case of the syn conformer (the signals of the anti do not split). Also shown are the signals of the four ortho hydrogens of the phenyls trans to anthraquinone (both syn and anti at $-120\text{ }^\circ\text{C}$) that split, at $-155\text{ }^\circ\text{C}$, into two 1:1 signals (only the left signals of two hydrogens are displayed) due to restricted phenyl rotation.

the restricted phenyl rotation that makes the ortho hydrogens diastereotopic in both the syn and anti conformers. The frozen phenyl rotation also accounts for the two unequally populated forms observed for the syn conformer at $-155\text{ }^\circ\text{C}$: these forms, in fact, are due to the two different dispositions that can be adopted by the frozen phenyl groups. Indeed, DFT computations predict that there are two such forms, corresponding to the two energy minima displayed in Figure 5. This feature is observed in the syn but not in the anti conformer: computations indicate in fact that the anti has only one minimum of energy (i.e., that reported in Figure 3): this agrees well with the experimental observation. Owing to the complex spectral appearance, due to the large number of overlapping lines, a quantitative line shape determination of the phenyl rotation rate was impossible and an approximate estimate of the barrier,¹³ based on the coalescence temperature, could be obtained solely for the pair

(13) Although in principle two different barriers should be observed for the phenyl rotation in the syn and anti conformers, this difference (which in any case is likely to be small) could not be appreciated since these low-temperature spectra did not exhibit sufficient details for this purpose.

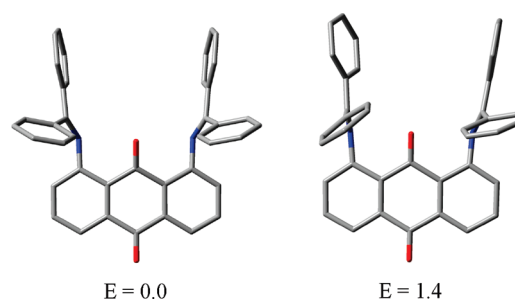


FIGURE 5. DFT-computed structures of the two possible conformations available to the conformer syn of **1**. The relative energies of the two minima are in kcal mol^{-1} (the structure with $E = 0.0$ is the same as that with $E = 0.0$ of Figure 3).

of phenyl groups in the position trans to the anthraquinone moiety¹⁴ ($\sim 5.8\text{ kcal mol}^{-1}$, as in Table 1).

The anthracene derivative **2** displays two diastereotopic phenyl groups (cis and trans to the anthracene ring) even at ambient temperature since in the ^1H spectrum two signals for the ortho, meta, and para hydrogens are visible. At higher temperatures these signals broaden and coalesce, eventually yielding averaged signals at about $+130\text{ }^\circ\text{C}$ (Figure S1, Supporting Information) since the two phenyl groups bonded to the $\text{C}=\text{N}$ moiety become equivalent due to the fast sp^2 nitrogen inversion. By line shape simulation it was found that the barrier is $16.2\text{ kcal mol}^{-1}$, the calculated value for this type of process being $15.1\text{ kcal mol}^{-1}$ according to DFT computations. The same calculations also predict that both the syn and anti conformers should be populated, having a computed energy difference of $0.26\text{ kcal mol}^{-1}$, and their interconversion barrier is calculated to be quite low (3.9 kcal mol^{-1}).

For this reason, we could observe separate NMR signals for the syn and anti conformers of **2** only below $-160\text{ }^\circ\text{C}$, where the ratio between the major and minor signals is about 86:14 at $-168\text{ }^\circ\text{C}$ (Figure 6). X-ray diffraction (Figure S2, Supporting Information) shows that the structure of **2** in the crystal is syn (as observed in **1**), whereas computations suggest that the anti should be slightly more stable (by $0.26\text{ kcal mol}^{-1}$). This discrepancy could be a consequence of the solvent effect, and therefore, we repeated the calculations by taking into account the effect of the solvent (CH_3CN) from which the compound had been crystallized. In this case, the computed energy difference between the two forms is essentially zero, thus proving that the solvent does play a role in determining the conformer proportions (furthermore, the computed energy differences are too small to allow a reliable assignment solely on theoretical grounds). Thus, the X-ray identification of a syn structure of **2** seems to be the most plausible assignment also for the more populated of the two conformers observed in solution. In addition, it is worth mentioning that a restricted rotation of the phenyl groups of the major conformer of **2** was observed, since the corresponding ortho and meta hydrogen signals (for both the pairs of phenyls cis and trans to anthracene) split into two, with a 1:1 ratio below $-165\text{ }^\circ\text{C}$.¹⁵ The two barriers for this

(14) The signals of the phenyl groups cis to anthraquinone are, in fact, overlapped by other spectral lines.

(15) The barriers were estimated at the coalescence temperature of the signals of the major conformer. In the coalescence region the signals of the minor conformer were not sufficiently intense to be observed.

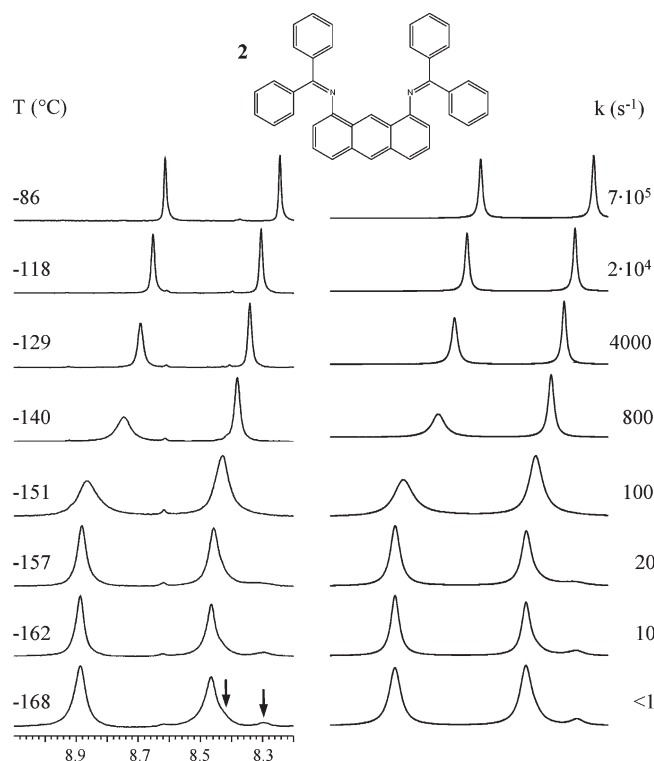


FIGURE 6. (Left) Low temperature ^1H signals of H9 and H10 of the anthracene moiety of **2** (600 MHz in $\text{CDCl}_2/\text{CBrF}_3$, 3:1). The arrows indicate the corresponding signals of the minor conformer (14%). (Right) Simulation obtained with the rate constants reported.

rotation process are slightly different, that involving the phenyl trans ($\sim 4.8 \text{ kcal mol}^{-1}$) being lower than that involving the phenyl cis ($\sim 5.4 \text{ kcal mol}^{-1}$), probably because the latter experiences a slightly larger steric hindrance. Since the latter barrier is almost equal, within the errors, to that of the Ar–N rotation (i.e., the syn/anti interconversion, 5.4 and 5.8 kcal mol^{-1} , respectively), it cannot be excluded that the cis phenyl signals actually monitor the same process displayed by the anthracene signals. Indeed, the calculated energy for the cis-phenyl rotation is higher than that of the Ar–N rotation (6.1 vs 3.9 kcal mol^{-1} , as in Table 1). If this is the case, the diastereotopicity of the ortho signals of the cis phenyl ring can be observed only when the Ar–N rotation is also frozen.¹⁶

Once again, the NMR spectrum of biphenylene derivative **3** shows that the two phenyl groups bonded to the N=C moiety are diastereotopic at ambient temperature, in that they display three pairs of ^1H NMR signals for the ortho, meta, and para hydrogens. These phenyls exchange their positions increasingly fast on warming, eventually yielding three averaged signals for the ortho, meta, and para hydrogens above +100 °C (Figure S3, Supporting Information).

(16) Such a situation, for instance, has been encountered in some aliphatic amines where the larger C–N rotation barrier is NMR invisible until the N-inversion, which has a lower barrier, is also frozen; see: Jackson, W. R.; Jennings, W. B. *Tetrahedron Lett.* **1974**, *15*, 1837–1838. See also: Anderson, J. E.; Casarini, D.; Ijeh, A. J.; Lunazzi, L. *J. Am. Chem. Soc.* **1997**, *119*, 8050–8057. Casarini, D.; Lunazzi, L.; Mazzanti, A.; Foresti, E. *J. Org. Chem.* **1998**, *63*, 4746–4754. Lunazzi, L.; Mazzanti, A.; Muñoz Alvarez, A. *J. Org. Chem.* **2000**, *65*, 3200–3206. Jewett, J. G.; Breyer, J. J.; Brown, J. H.; Bushweller, C. H. *J. Am. Chem. Soc.* **2000**, *122*, 308–323.

The experimental barrier for the planar nitrogen inversion, as obtained from the line shape analysis, is 17.3 kcal mol^{-1} (Table 1). According to calculations, the anti conformer of **3** is more stable than the syn by 0.92 kcal mol^{-1} , in agreement with the X-ray structure that, contrary to the case of compounds **1** and **2**, shows that the structure anti is adopted in the crystalline state (Figure S2, Supporting Information).

The barrier calculated by DFT computations for the syn/anti interconversion due to Ar–N rotation is too low (2.7 kcal mol^{-1}) to allow an experimental determination by variable-temperature NMR, and indeed, the spectra of **3** do not display the effects of this process even at -165 °C . On the other hand, the restricted phenyl rotation, which renders diastereotopic the corresponding ortho hydrogens, was observed, as in the case of **1** and **2**.

It should be noted that the rotation barriers for the trans and the cis phenyl rings are both calculated to be higher than that for the Ar–N rotation (5.2 and 5.2 vs 2.7 kcal mol^{-1} , as in Table 1). The rotational process of the trans phenyl is visible even in the presence of a fast Ar–N rotation, whereas this is not the case for the rotation of the cis phenyl group. For this reason, the barrier for the phenyl rotational process could be determined solely for the phenyl groups trans to biphenylene ($\sim 5.6 \text{ kcal mol}^{-1}$ at the coalescence temperature, as in Table 1).

In addition, compound **4** displays at ambient temperature diastereotopic cis and trans phenyl groups, but in this case, they belong solely to a single conformer. There is no evidence, in fact, of the existence of a second conformer, even at very low temperature (see, for instance, the naphthalene signal of the hydrogens in position 2,7 in Figure S4 of the Supporting Information). The anti structure was assigned to the observed conformer because DFT calculations predict the syn to be less stable than the anti by as much as 5.4 kcal mol^{-1} . Due to the proximity of the α positions 1,8 of naphthalene, the N=CPh₂ groups bonded to these positions are very crowded in the syn situation, hence accounting for the much lower stability of this conformer with respect to the anti. Such a theoretical assignment is further supported by the X-ray diffraction which shows that in the solid state the molecule adopt indeed the anti structure (Figure S5, Supporting Information).

At higher temperatures, the fast N-inversion process is expected to eliminate the diastereotopicity of the phenyl groups. For instance, the two ortho ^1H signals of the phenyl groups coalesce into a single signal at +65 °C (Figure S6, Supporting Information), the corresponding barrier being 16.6 kcal mol^{-1} .

In the low-temperature NMR spectra of **4** the effects of the restricted rotation of the phenyl groups, both in the cis and trans position, were observed, with experimental barriers lower than that predicted by calculations for the Ar–N rotation. In Figure S4 of the Supporting Information, the signal at 7.47 ppm (for the four ortho hydrogens of the two phenyls cis) splits at -141 °C into two equal signals, with a separation of 265 Hz at 600 MHz (the coalescence temperature is about -120 °C). The signal at 7.31 ppm (corresponding to the four ortho hydrogens of the two phenyls trans) similarly splits at -162 °C with a separation of 670 Hz at 600 MHz (the coalescence temperature is about -145 °C). From these data an approximate estimate of the two barriers could be determined (~ 6.9 and $\sim 5.4 \text{ kcal mol}^{-1}$, respectively, as

in Table 1). As conceivable, the rotation barrier of the trans phenyls is lower than that of the cis, presumably because the latter are more hindered, owing to the proximity to the naphthalene ring.

Conclusions

It has been shown that 1,8-aryldiimino derivatives of anthraquinone, anthracene, biphenylene, and naphthalene are not planar, and for this reason they can originate syn and anti conformers. The interconversion barriers involving N-inversion and Ar–N bond rotation have been determined by variable-temperature NMR spectroscopy. DFT calculations indicate that the preferred conformer switches from syn to anti on reducing the distance between the nitrogen atoms, a result supported by X-ray diffraction analysis.

Experimental Section

Materials. 1,8-Dichloroanthraquinone, diphenylmethanimine, and Xantphos were commercially available. 1,8-dibromoanthracene,¹⁷ 1,8-dibromobiphenylene,¹⁸ and 1,8-diiodonaphthalene¹⁹ were prepared following known procedures.

General Procedure for 1–4.²⁰ To a solution of the appropriate 1,8-dihalogen compound (10 mmol, in 20 mL dry toluene) were added Pd₂(dba)₃ (2 mol %, 192 mg), Xantphos (4 mol %, 231 mg), and NaO-*t*-Bu (30 mmol, 2.805 g) at room temperature, and the solution was stirred for 30 min. Then diphenylmethanimine (23 mmol, 4.168 g, 3.87 mL) was added and the solution heated at 100 °C for 24 h. After the solution was cooled at room temperature, the organic layer was extracted with EtO₂ and dried with Na₂SO₄. The solvent was evaporated, and the crude products were purified by chromatography on silica gel (hexane/Et₂O mixture 10:1 v/v) to obtain a mixture containing mainly the 1-chloro-8-(diphenylmethyleneamino) derivative and the target product. The mixture was separated by preparative HPLC (see the Supporting Information for details). The isolated 1-chloro-8-(diphenylmethyleneamino) intermediates were then reacted as above to yield a second batch of the products (total yields: 56% for **1**, 62% for **2**, 58% for **3**, 18% for **4**). Crystals suitable for X-ray diffraction analyses were obtained by slow evaporation of acetonitrile solutions. Spectroscopic and analytical data are reported in the Supporting Information.

NMR Spectroscopy. The spectra were recorded at 600 MHz for ¹H and 150.8 MHz for ¹³C. The assignments of the ¹H and ¹³C signals were obtained by bidimensional experiments (edited-gHSQC²¹ and gHMBC²² sequences). The NOE experiments on **3** were obtained by means of the DPFGE-NOE²³ sequence. To selectively irradiate the desired signal, a 50 Hz wide shaped pulse was calculated with a refocusing-SNOB shape²⁴ and a pulse width of 37 ms. The mixing time was set to 1.5 s. Temperature calibrations were performed before the experiments, using a Cu/Ni thermocouple immersed in a dummy sample tube filled with 1,1,2,2-tetrachloroethane for the high temperature or isopentane for the low temperature range, and under conditions as nearly identical as possible. The uncertainty in the temperatures was estimated from the calibration curve to be ±1 °C. The line shape simulations were performed by means of a PC version of the QCPE program DNMR 6 no. 633, Indiana University, Bloomington, IN.

Calculations. Geometry optimizations were carried out at the B3LYP/6-31G(d)²⁵ level by means of the Gaussian 03 series of programs²⁶ (see the Supporting Information): the standard Berny algorithm in redundant internal coordinates and default criteria of convergence were employed. The energies reported in Table 1 are not ZPE corrected; full thermochemistry-corrected data are reported in the Supporting Information. Harmonic vibrational frequencies were calculated for all the stationary points. For each optimized ground state the frequency analysis showed the absence of imaginary frequencies, whereas each transition state showed a single imaginary frequency. Visual inspection of the corresponding normal mode²⁷ was used to confirm that the correct transition state had been found.

Acknowledgment. L.L. and A.M. received financial support from the University of Bologna (RFO) and from MIUR, Rome (PRIN national project “Stereoselection in Organic Synthesis, Methodologies and Applications”). Dr. M. Di Mattia, Sigma-Tau, Rome, is gratefully acknowledged for the acquisition of the ESI-TOF mass spectra.

Supporting Information Available: High-temperature VT spectra of **2–4**; low-temperature VT spectra of **4**; spectroscopic and analytical data, X-ray structures, ¹H, ¹³C NMR spectra, computational data of **1–4**. This material is available free of charge via the Internet at <http://pubs.acs.org>.

(24) Kupčė, E.; Boyd, J.; Campbell, I. D. *J. Magn. Reson. Ser. B* **1995**, *106*, 300–303.

(25) Becke, A. D. *J. Chem. Phys.* **1993**, *98*, 5648–5652. Lee, C.; Yang, W.; Parr, R. G. *Phys. Rev. B* **1988**, *37*, 785–789. Stephens, P. J.; Devlin, F. J.; Chabalowski, C. F.; Frisch, M. J. *J. Phys. Chem.* **1994**, *98*, 11623–11627.

(26) Frisch, M. J.; Trucks, G. W.; Schlegel, H. B.; Scuseria, G. E.; Robb, M. A.; Cheeseman, J. R.; Montgomery, J. A., Jr.; Vreven, T.; Kudin, K. N.; Burant, J. C.; Millam, J. M.; Iyengar, S. S.; Tomasi, J.; Barone, V.; Mennucci, B.; Cossi, M.; Scalmani, G.; Rega, N.; Petersson, G. A.; Nakatsuji, H.; Hada, M.; Ehara, M.; Toyota, K.; Fukuda, R.; Hasegawa, J.; Ishida, M.; Nakajima, T.; Honda, Y.; Kitao, O.; Nakai, H.; Klene, M.; Li, X.; Knox, J. E.; Hratchian, H. P.; Cross, J. B.; Bakken, V.; Adamo, C.; Jaramillo, J.; Gomperts, R.; Stratmann, R. E.; Yazyev, O.; Austin, A. J.; Cammi, R.; Pomelli, C.; Ochterski, J. W.; Ayala, P. Y.; Morokuma, K.; Voth, G. A.; Salvador, P.; Dannenberg, J. J.; Zakrzewski, V. G.; Dapprich, S.; Daniels, A. D.; Strain, M. C.; Farkas, O.; Malick, D. K.; Rabuck, A. D.; Raghavachari, K.; Foresman, J. B.; Ortiz, J. V.; Cui, Q.; Baboul, A. G.; Clifford, S.; Cioslowski, J.; Stefanov, B. B.; Liu, G.; Liashenko, A.; Piskorz, P.; Komaromi, I.; Martin, R. L.; Fox, D. J.; Keith, T.; Al-Laham, M. A.; Peng, C. Y.; Nanayakkara, A.; Challacombe, M.; Gill, P. M. W.; Johnson, B.; Chen, W.; Wong, M. W.; Gonzalez, C.; Pople, J. A. *Gaussian 03, Revision E.01*; Gaussian, Inc.: Wallingford, CT, 2004.

(27) Gaussview 4.1.2; Gaussian, Inc.: Wallingford, CT, 2006

(17) Pérez-Trujillo, M.; Maestre, I.; Jaime, C.; Alvarez-Larena, A.; Pinella, J. F.; Virgili, A. *Tetrahedron: Asymmetry* **2005**, *16*, 3084–3093.

(18) Humayun Kabir, S. M.; Hasegawa, M.; Kuwatani, Y.; Yoshida, M.; Matsuyama, H.; Iyoda, M. *J. Chem. Soc., Perkin Trans. 1* **2001**, 159–165. For the preparation of the intermediate 2,2',6,6'-tetrabromobiphenyl, see: Rajca, A.; Safronov, A.; Rajca, S.; Ross, C. R. II; Stezowski, J. J. *J. Am. Chem. Soc.* **1996**, *118*, 7272–7279.

(19) House, H. O.; Koepsell, D. G.; Campbell, W. J. *J. Org. Chem.* **1972**, *37*, 1003–1011.

(20) Grossman, O.; Rueck-Braun, K.; Gelman, D. *Synthesis* **2008**, 537–542.

(21) Bradley, S. A.; Krishnamurthy, K. *Magn. Reson. Chem.* **2005**, *43*, 117–123. Willker, W.; Leibfritz, D.; Kerssebaum, R.; Bermel, W. *Magn. Reson. Chem.* **1993**, *31*, 287–292.

(22) Hurd, R. E.; John, B. K. *J. Magn. Reson.* **1991**, *91*, 648–653.

(23) Stonehouse, J.; Adell, P.; Keeler, J.; Shaka, A. J. *J. Am. Chem. Soc.* **1994**, *116*, 6037–6038. Stott, K.; Stonehouse, J.; Keeler, J.; Hwang, T. L.; Shaka, A. J. *J. Am. Chem. Soc.* **1995**, *117*, 4199–4200. Stott, K.; Keeler, J.; Van, Q. N.; Shaka, A. J. *J. Magn. Reson.* **1997**, *125*, 302–324. Van, Q. N.; Smith, E. M.; Shaka, A. J. *J. Magn. Reson.* **1999**, *141*, 191–194.